Bioorganic & Medicinal Chemistry Letters 19 (2009) 1403–1408

Contents lists available at ScienceDirect

Bioorganic & Medicinal Chemistry Letters

journal homepage: www.elsevier.com/locate/bmcl

N-Hydroxy-1,2-disubstituted-1*H*-benzimidazol-5-yl acrylamides as novel histone deacetylase inhibitors: Design, synthesis, SAR studies, and in vivo antitumor activity

Haishan Wang *, Niefang Yu, Hongyan Song, Dizhong Chen, Yong Zou, Weiping Deng, Pek Ling Lye, Joyce Chang, Melvin Ng, Stéphanie Blanchard, Eric T. Sun, Kanda Sangthongpitag, Xukun Wang, Kee Chuan Goh, Xiaofeng Wu, Hwee Hoon Khng, Lijuan Fang, Siok Kun Goh, Wai Chung Ong, Zahid Bonday, Walter Stünkel, Anders Poulsen, Michael Entzeroth

*S*BIO Pte Ltd, 1 Science Park Road, #05-09 The Capricorn, Singapore Science Park II, Singapore 117528, Singapore*

ARTICLE INFO

Article history:
Received 25 November 2008
Revised 9 January 2009
Accepted 13 January 2009
Available online 19 January 2009

Keywords:
HDAC inhibitor
Benzimidazole
Hydroxamic acid
SAR
Anticancer

ABSTRACT

A series of *N*-hydroxy-1,2-disubstituted-1*H*-benzimidazol-5-yl acrylamides were designed and synthesized as novel HDAC inhibitors. General SAR has been established for the substituents at positions 1 and 2, as well as the importance of the ethylene group and its attachment to position 5. Optimized compounds are much more potent than SAHA in both enzymatic and cellular assays. A representative compound, **23** (SB639), has demonstrated antitumor activity in a colon cancer xenograft model.

© 2009 Elsevier Ltd. All rights reserved.

The amino termini of histones extend from the nucleosomal core and are modified by histone acetyltransferases (HATs) and histone deacetylases (HDACs) during the cell cycle.[1] Acetylation of the ε-amino groups of lysine residues removes positive charges, thereby reducing the affinity between histones and negatively charged DNA. This facilitates access of the transcriptional machinery to the DNA template. Therefore, in most cases, histone acetylation enhances transcription while histone deacetylation represses transcription.[2,3] Inhibition of HDACs results in the accumulation of acetylated histones, which results in a variety of cell type dependent responses, such as apoptosis, necrosis, differentiation, cell survival, inhibition of proliferation and cytostasis. HDAC inhibitors (HDACi) have been studied for their therapeutic effects on cancer cells.[4] Suberoylanilide hydroxamic acid (SAHA, Vorinostat), the first HDACi approved by the FDA in 2006 for the treatment of cutaneous T-cell lymphoma, validates HDAC inhibition as a strategy for cancer therapy.[5]

HDAC enzymes are divided into four different classes.[6] Class I and II isozymes, specifically HDAC 1, 2, 3, 6 and 8, have been associated with uncontrolled tumor growth. For example, selective knockdown studies on HDACs suggest that the class I HDACs, particularly HDACs 1 and 3, are essential to the proliferation and survival of mammalian carcinoma cells.[7]

There are a number of HDACi which are currently undergoing clinical trials either as a single therapy or in combination for treatment of solid and hematologic malignancies (Fig. 1). The mor-

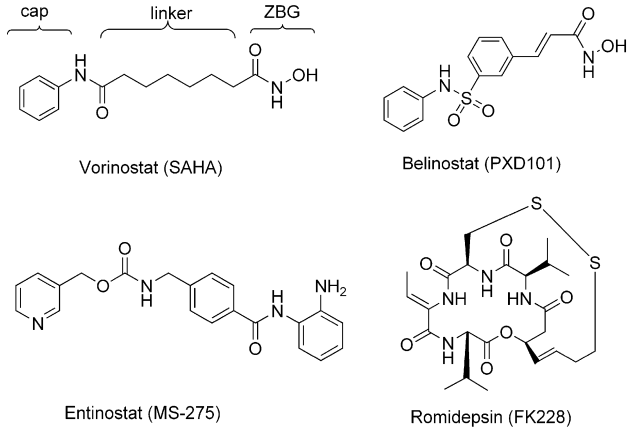

Figure 1. Examples of clinically tested HDAC inhibitors.

* Corresponding author. Tel.: +65 68275019; fax: +65 68275005.
E-mail address: haishan_wang@sbio.com (H. Wang).

0960-894X/$ - see front matter © 2009 Elsevier Ltd. All rights reserved.
doi:10.1016/j.bmcl.2009.01.041

phology of the HDACi pharmacophore is characterized by three portions: cap, linker and zinc-binding group (ZBG) as exemplified by SAHA (Fig. 1). The common linkers are aliphatic chain (e.g., six carbon chain in SAHA), aromatic ring (e.g., phenylene in MS-275)[8] and vinyl-aromatic (e.g., styryl in PXD101).[9] The most common ZBGs are hydroxamic acid and benzamide (e.g., MS-275). Hydroxamic acid remains among the most potent and popular ZBGs reported for inhibition of Class I HDACs.

As part of our ongoing effort to discover novel anticancer agents, we have examined a number of fused heterocyclic rings such as benzimidazole, benzothiophene, indole and indazole as part of a novel linker or building block for a low molecular weight novel HDACi. In this report, we describe the development of *N*-hydroxy-1,2-disubstituted-1*H*-benzimidazol-5-yl acrylamides (**VII**) (Scheme 1), a series of novel HDACi with promising pharmacological and pharmacokinetic properties.

The X-ray structures of HDLP (histone deacetylase like protein) co-crystallized with SAHA and trichostatin A indicate that a linker incorporating a pi-system is preferred for interaction with two phenyl groups in the binding pocket (Phe198 and Phe141).[10] Docking studies revealed that vinyl-aromatic rings are suitable linkers.[11] We envisaged that **VII**, with appropriately substituted groups R^1 and R^2, would have additional interactions with protein residues in the 'cap' region.

An efficient synthesis of a wide range of benzimidazole-based hydroxamic acids was developed. Scheme 1, Route A, illustrates the general procedure used for preparing hydroxamic acids (**VII**), starting from *trans*-3-nitro-4-chloro-cinnamic acid (**I**) in a 4-step

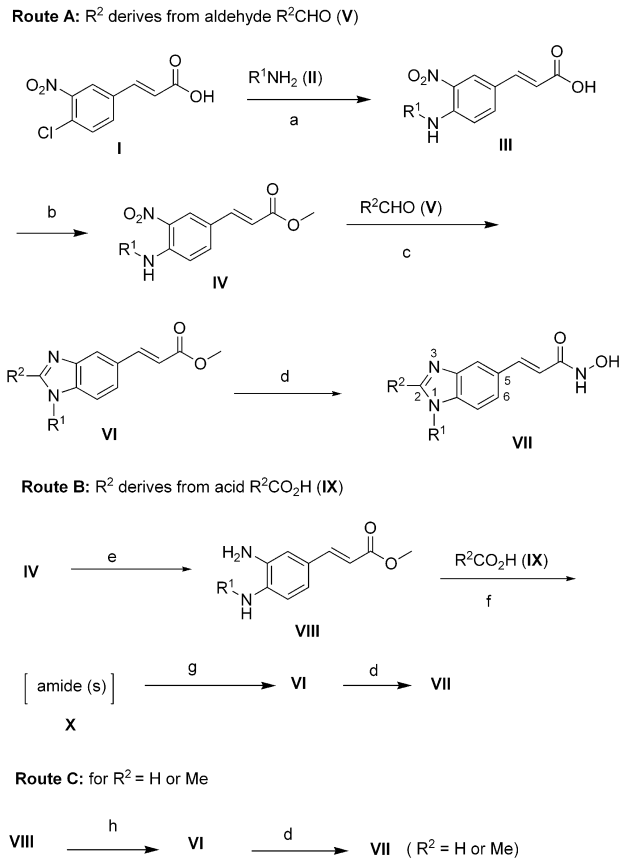

Scheme 1. Reagents and conditions: (a) Et_3N, dioxane, 100 °C; (b) MeOH,H_2SO_4, 60 °C; (c) $SnCl_2{\cdot}2H_2O$ (5 equiv), AcOH/MeOH (1:9), 40 °C; (d) $NH_2OH{\cdot}HCl$ (10 equiv)/NaOMe (20 equiv)/MeOH, 0 °C to rt; (e) $SnCl_2{\cdot}2H_2O$ (5 equiv), AcOH/MeOH (1:9), 40 °C; (f) coupling reagent (EDCI), HOBt; (g) HOAc, reflux; (h) HCO_2H or CH_3CO_2H, reflux.

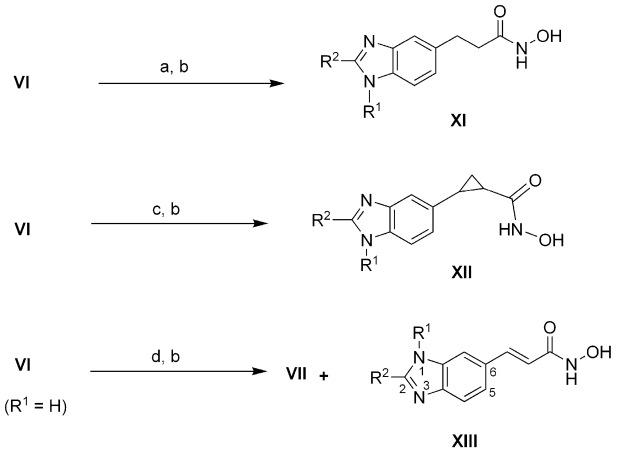

Scheme 2. Reagents and conditions: (a) H_2 (1 atm)/10% Pd–C, rt, (b) $NH_2OH{\cdot}HCl$ (10 equiv)/NaOMe (20 equiv)/MeOH, 0 °C to rt; (c) $(CH_3)_3S(O)I$, NaH, THF, rt, Et_2O; (d) R^1X (X = I, Br), K_2CO_3, CH_3CN.

reaction sequence. Chloride displacement by amine R^1NH_2 (**II**) under basic conditions, followed by esterification of the acid (**III**) gave methyl ester (**IV**). Alternatively, **I** may be esterified to the methyl ester (**Ia**) first, followed by installation of amine (**II**) to give **IV**. One-pot reductive cyclization of **IV** with aldehyde (**V**) forms the benzimidazole ring.[12] In this key step, the nitro group of **IV** was reduced by tin (II) chloride in acetic acid, and in the presence of aldehyde (**V**) ring cyclization was achieved to give benzimidazole (**VI**) in 40–65% yield. Treatment of the methyl ester (**VI**) with excessive hydroxylamine gave hydroxamates (**VII**) in good yield.[13] If the desired aldehyde (**V**) was not readily available, acid (**IX**) was used for formation of amide (**X**) first, then cyclized to benzimidazole (**VI**) under acidic conditions [14] (Scheme 1, Route B). **VII** (R^2 = H or Me) can be obtained by refluxing formic acid or acetic acid, respectively, with diamine (**VIII**) (Scheme 1, Route C).

To assess the role of the olefinic linker between the zinc-binding hydroxamic acid and the fused aromatic ring, the saturated alkyl linker analog (**XI**) and a cyclopropyl analog (**XII**) were prepared as illustrated in Scheme 2. Alkylation of **VI** (R^1 = H) with R^1X (e.g., benzyl bromide, MeI) provided two products after separation: one was identical to an authentic sample (**VII**) prepared as in Scheme 1, the other was the isomer **XIII**.

Initially synthesized analogs, with R^1 fixed as a propanol group, were profiled against the HDAC1 enzyme and the human colon cancer cell line COLO205 (Table 1).[15,16] The propanol group was selected as R^1 with the expectation of possible interactions between it and the hydrophilic side-chains in HDAC1, for example, Asp 99 or Glu 98.[10] R^2 was optimized with a range of groups: unsubstituted (**1**), aromatic and non-aromatic rings (**2** and **3**), straight and branched alkyl chains (**4**, **5 and 6**) and arylalkyl chains (**7**, **8** and **9**). Compounds with a directly attached ring or an α-branch (**2**, **3** and **4**) were not potent, but those with α-unsubstituted phenylalkyl chains (**7**, **8** and **9**) were not only potent in the HDAC1 enzyme assay, but also in a cellular anti-proliferation assay using colon cancer cell line COLO 205.

To investigate the role of the R^1 substituent, a series of compounds were synthesized in which R^2 was held constant as phenethyl while varying R^1. Phenethyl was selected as R^1 substituent because it has reasonable contribution to in vitro potency, is simpler and achiral compared to 2-phenyl-propyl in **8**. A number of R^1 substituents were explored for size (both linear and bulky), lipophilicity and hydrophilicity (neutral, acidic and basic) and combinations of the above (Table 2). Hydrophobic and bulky groups are preferred for R^1 with a short flexible linker (m = 1, **13** vs **12** and **11**). For R^1 substituents with a longer flexible linker

Table 1
SAR of R^2 for **VII** with R^1 = –$(CH_2)_3$–OH fixed

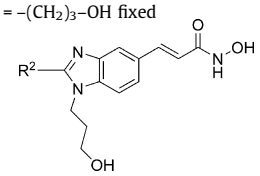

Compound	R^2	HDAC1 IC_{50}[a] (μM)	COLO 205 IC_{50}[b] (μM)
1	H	1.10 ± 0.14	Not tested
2		3.2[c]	31[c]
3		1.9[c]	31[c]
4		1.70 ± 0.36	Not tested
5		0.10 ± 0.05	26 ± 17
6		0.53[c]	3.7 ± 0.1
7		0.17[c]	3.2 ± 0.1
8		0.08 ± 0.04	1.7 ± 0.6
9	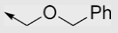	0.17[c]	4.1 ± 1.9

[a] Values are expressed as mean ± standard deviation of at least two independent duplicate experiments.
[b] Values are expressed as mean ± standard deviation of at least two independent triplicate experiments.
[c] Values obtained from only one duplicate or triplicate experiment.

(m = 2 and 3), none of the acidic (**15**), cyclic amide (**20**) or lipophilic groups (**17**) enhanced HDAC1 or cell proliferation inhibition. Even though potencies of compounds with linear chains (**7**, **14**, **18** and **19**) were comparable to those with basic chains (**16** and **21**), the basic R^1 side-chains were chosen for further optimization due to their higher aqueous solubility.

Table 2
SAR of R^1 = –$(CH_2)_m$–Y for **VII** with R^2 = –$(CH_2)_2$–Ph fixed

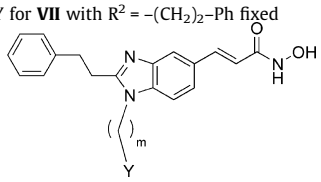

Compound	m	Y	HDAC1 IC_{50}[a] (μM)	COLO 205 IC_{50}[b] (μM)
10	0	H	0.17 ± 0.01	4.4 ± 2.2
11	1	H	0.26 ± 0.14	1.2 ± 0.6
12	1	Ph	0.41 ± 0.06	1.6 ± 0.8
13	1	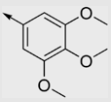	0.047 ± 0.013	0.32 ± 0.21
14	2	H	0.22 ± 0.05	1.5 ± 0.5
15	2	CO_2H	2.3 ± 0.4	Not tested
16	2	Morpholin-4-yl	0.27 ± 0.07	2.8 ± 0.3
17	2	Ph	0.88[c]	8.8 ± 0.8
18	3	H	0.17 ± 0.07	2.3 ± 0.5
7	3	OH	0.17[c]	3.2 ± 0.1
19	3	OCH_3	0.21[c]	2.2 ± 0.3
20	3		0.20 ± 0.02	11 ± 4
21	3	Morpholin-4-yl	0.25 ± 0.06	1.9 ± 0.9

[a,b,c] See footnote of Table 1.

Table 3
SAR of R^1 = amines for **VII** with R^2 = –$(CH_2)_2$–Ph fixed

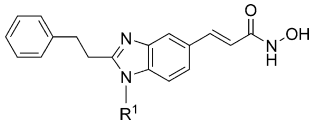

Compound	R^1	HDAC1 IC_{50}[a] (μM)	COLO 205 IC_{50}[b] (μM)
22	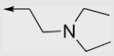	0.052 ± 0.025	0.22 ± 0.12
23 (SB639)	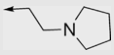	0.035 ± 0.016	0.14 ± 0.05
24	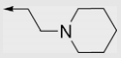	0.026 ± 0.014	0.09 ± 0.06
25	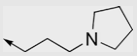	0.31 ± 0.21	0.61 ± 0.26
26	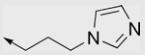	0.16 ± 0.06	>100
27	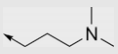	0.19 ± 0.01	2.0 ± 1.1
28	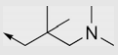	0.041 ± 0.019	0.12 ± 0.07
29	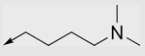	0.16 ± 0.04	1.1 ± 0.2

[a,b] See footnote of Table 1.

Hence, a series of compounds with basic R^1 side-chains were synthesized (Table 3). Both enzymatic and cellular activities were significantly improved with a mono basic amine with a two carbon linker (**22**, **23** and **24**). Compounds with longer linkers of three carbons and more were less potent (**23** vs **25**, **27** and **29**). Increasing lipophilicity of the amine substituent improved potency slightly (**24** vs **23**). Docking compound **23** into the HDAC1 homology model[17,18] revealed a key electrostatic interaction between the R^1 basic center and Asp99 (Fig. 2). There is an additional hydrogen bonding interaction between the hydroxyl of Tyr204 and benzimidazole N3, thus both basic centers contribute to the binding of the most potent compounds, such as **22**, **23** and **24**. Compounds with longer linkers (**25**, **26**, **27** and **29**), due to their increased distance between R^1 basic center and Asp99 according to the binding mode of **23**, have to fold back their R^1 side-chains in order to make similar interactions with Asp99, but the overall bindings become less effective. However, **28**, has a bulky *gem*-dimethyl group in R^1

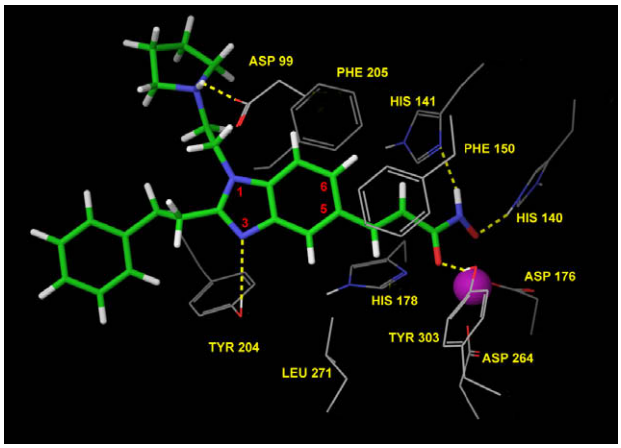

Figure 2. Compound **23** (SB639) docked into the HDAC1 homology model. Key interactions between the basic centers with Asp99 and Tyr204 contribute to the potency.

Table 4
SAR of Z for **XIV**

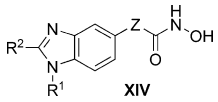

XIV

Compound	R^1	R^2	Z	HDAC1 IC_{50}[a] (μM)	COLO 205 IC_{50}[b] (μM)
5			–CH=CH–	0.10 ± 0.05	26 ± 17
30			$-CH_2CH_2-$	>10	Not tested
7			–CH=CH–	0.17[c]	3.2 ± 0.1
31			– (bond)	3.3[c]	26 ± 1
13	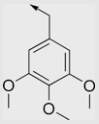		–CH=CH–	0.047 ± 0.013	0.32 ± 0.21
32			$-CH_2CH_2-$	0.17 ± 0.00	2.4 ± 0.5
11	CH_3		–CH=CH–	0.26 ± 0.14	1.2 ± 0.6
33				1.3 ± 1.0	Not tested

[a,b,c] See footnote of Table 1.

side-chain which can force it to adopt favorable conformation(s) to make effective interaction with Asp99 explaining its high potency.

Assessment of the role of the linker between the zinc-binding hydroxamic acid and the benzimidazole ring was explored with compounds made according to Scheme 2 (biological data listed in Table 4). Saturation of the double bond either reduced HDAC1 potency 3.6-fold (**32** vs **13**) or destroyed it completely (**30** vs **5**). Clearly the nature of specific side-chains in combination with the Z linker is crucially important. The cyclopropyl moiety, as a replacement for ethylene (**33**) lost 5-fold potency perhaps due to an unfavorable hydrophobic interaction or conformational change. When the hydroxamic acid is directly attached to the benzimidazole ring (**31**, which was made by using method analogous to Route A, Scheme 1 and 4-chloro-3-nitro-benzoic acid methyl ester as starting material instead of **I**), inhibition of HDAC1 enzyme activity was reduced by over an order of magnitude (**31** vs **7**).

The position of attachment of the alkenoyl hydroxamate to the benzimidazole ring at either position 5 or 6 was explored with the pair of compounds **34** (Table 5) and **12**. The 5-substituted compound **12** is more potent against HDAC1. Illustrating the superior

Table 5
Isomeric benzimidazole and benzamides

Compound	Structures	HDAC1 IC_{50}[a] (μM)	COLO 205 IC_{50}[a] (μM)
12		0.41 ± 0.06	1.6 ± 0.8
34		1.2 ± 0.2	5.4 ± 0.5
35	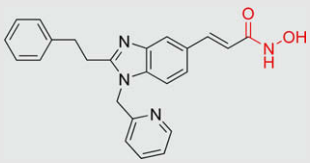	0.25 ± 0.25	0.88 ± 0.46
36	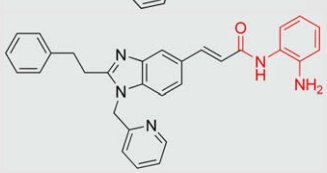	>100	5.1 ± 2.6

[a,b] See footnote of Table 1.

Table 6
Cellular IC_{50} (μM) of selected compounds

Compound	HCT116	A2780	PC3
11	1.3 ± 0.3	0.73 ± 0.04	0.89 ± 0.23
22	0.24 ± 0.09	0.10 ± 0.00	0.20 ± 0.09
23	0.20 ± 0.10	0.19 ± 0.14	0.15 ± 0.08
24	0.10 ± 0.03	0.031 ± 0.000	0.12 ± 0.04
28	0.16 ± 0.10	0.11 ± 0.00	0.18 ± 0.08

Table 7
Half-life $T_{1/2}$ (min) in liver microsomal stability assay[19]

Compound	Human	Mouse
11	>30	23 ± 3
22	16 ± 5	2.8 ± 1.7
23	>30	2.7 ± 2.0
24	10 ± 1	1.3 ± 0.5
28	12 ± 1	1.0 ± 0.0

potency of the hydroxamate ZBG, **35** is a much more potent HDAC1 inhibitor than the corresponding benzamide (**36**). The above results clearly demonstrate that the properties of the side-chains and their positions of substitution on the benzimidazole ring are crucial for optimal enzyme and cellular potency.

The most promising compounds representing different R^1 side-chains were selected for further evaluation in cell lines and in vivo. Broad activity against other human tumor cell lines, such as HCT116, A2780 and PC3 was encouraging (Table 6).[16]

Given the good cellular activity in vivo xenograft studies were initiated in HCT116 tumor-bearing nude mice (10 mice per dose group). Considering their low metabolic stability in mouse (Table 7), compounds were given daily ip at doses up to MTD (maximum tolerated dose).[20] **22**, **23**, **24** and **28** were dosed as the di-hydrochloride salt and **11** as the mono-hydrochloride. **23** demonstrated significant antitumor activities compared to vehicle control, tumor growth inhibition (TGI) on day 22 was 89% (130 mg/kg, MTD, $p < 0.01$, maximum body weight loss (MBWL): 8.7% on day 19) and 59% (70 mg/kg, $p < 0.01$, MBWL: 0.5% on day 15) (Fig. 3). SAHA (IC_{50} = 0.12 ± 0.04 and 2.9 ± 1.6 μM for HDAC1 and HCT116, respectively) was used as a positive control and showed moderate activity at 200 mg/kg (MTD) with TGI = 53% ($p < 0.01$).

The antitumor activities of **11**, **22** and **24** were not significantly different from vehicle controls ($p > 0.05$) in other experiments. The TGIs were 23% (50 mg/kg, qdx21, MTD) and 32% (75 mg/kg, qdx21, MTD) on day 21 for **11** and **24**, respectively. The TGI on day 22 was 12% for **22** (60 mg/kg, qdx21, MTD). Compound **28** was not tolerated in nude mice even at the lowest dose tested (100 mg/kg), treatment ended on day 12, 2/10 and 1/10 treatment-related deaths occurred on days 13 and 14, respectively. The TGI on day 11 was 60% (100 mg/kg, $p > 0.05$), no further evaluation was done at lower doses.

Compound **23** was also given orally to tumor-bearing mice, with TGI on day 21 of 78% (200 mg/kg, qdx21, $p < 0.001$, MBWL: 5.7% on day 7) and 43% (100 mg/kg, qdx21, $p < 0.05$, no body weight loss). Pharmacokinetic studies have determined that compound **23** has an oral bioavailability in mouse of 13%.[19] When dosed at 50 mg/kg (po), the C_{max} (0.92 ± 0.05 μM),[19] was well above the IC_{50} levels for HDAC1 (0.035 ± 0.016 μM) and HCT116 (0.20 ± 0.10 μM). Plasma concentration was maintained above the HDAC IC_{50} for about 4 h. Given that the doses in the HCT116 xenograft experiment were much higher than this PK study it is not surprising that such good efficacy was seen.

The mechanism of action of **23** was confirmed both in vitro and in vivo as evidenced by hyperacetylation of H3 in HCT116 cells and tumor tissues after treatment with **23** (data not shown). **23** is also a

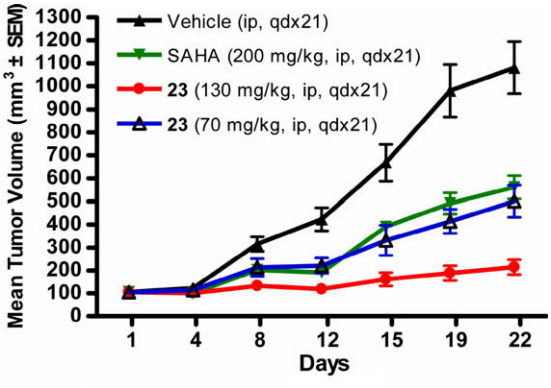

Figure 3. Antitumor activity of **23** in mouse HCT116 xenograft model

Table 8
SB639 (**23**) is a pan-HDAC inhibitor

HDAC[a]	K_i[b] (nM)	HDAC[a]	K_i[b] (nM)
1	11.6 ± 0.3	6	20.6 ± 0.8
2	36.2 ± 5.3	8	82 ± 9
3	12.5 ± 1.7	9	19.2 ± 1.1
4	9.6 ± 0.4	10	18.9 ± 1.1
5	17.2 ± 2.9	11	12.8 ± 2.5

[a] HDAC isoenzymes (HDAC7 not tested).
[b] Dissociation constant.[15]

potent pan-HDAC inhibitor, it inhibits class I, II and IV HDAC isoenzymes (Table 8). The basic nitrogens in **23** are not only essential for HDAC inhibition, but also for physicochemical properties. The hydrochloride salt of **23** has good solubility in mildly acidic media (1.6 mg/mL at pH 6.5) and lipophilicity at neutral pH in the ideal range ($\log D = 2.1$ at pH 7.3).

In conclusion, we have designed and synthesized a series of *N*-hydroxy-1,2-disubstituted-1*H*-benzimidazol-5-yl acrylamides, which exhibit potent enzymatic and cellular activity. A representative compound, **23** (SB639), exhibited excellent antitumor efficacy in an HCT116 xenograft model. Compound **23** was also orally active demonstrating the good drug-like properties from this template. Future reports will build on the SAR of the benzimidazole core structure with a view to delivering a clinical candidate.

Acknowledgments

We thank the S*BIO sample management team for preparing sample solutions for assays, the PKDM department for DMPK studies on **23**,[19] and Dr. Brian W. Dymock for critical review of the manuscript.

References and notes

1. Grunstein, M. *Nature* **1997**, *389*, 349.
2. Struhl, K. *Genes Dev.* **1998**, *12*, 599.
3. Wade, P. A. *Hum. Mol. Genet.* **2001**, *10*, 693.
4. Butler, L. M.; Agus, D. B.; Scher, H. I.; Higgins, B.; Rose, A.; Cordon-Cardo, C.; Thaler, H. T.; Rifkind, R. A.; Marks, P. A.; Richon, V. M. *Cancer Res.* **2000**, *60*, 5165.
5. Zolinza™ (SAHA, Vorinostat) was approved for the treatment of patients with cutaneous T-cell lymphoma who have progressive, persistent or recurrent disease on or following two systemic therapies, see FDA approval documents: http://www.fda.gov/cder/foi/nda/2006/021991s000_ZolinzaTOC.htm.
6. (a) De Ruijter, A. J. M.; van Gennip, A. H.; Caron, H. N.; Kemp, S.; van Kuilenburg, A. B. P. *Biochem. J.* **2003**, *370*, 737; (b) Michan, S.; Sinclair, D. *Biochem. J.* **2007**, *404*, 1.
7. (a) Curtin, M.; Glaser, K. *Curr. Med. Chem.* **2003**, *10*, 2373; (b) Glaser, K. B.; Li, J.; Staver, M. J.; Wei, R.-Q.; Albert, D. H.; Davidsen, S. K. *Biochem. Biophys. Res. Commun.* **2003**, *310*, 529.

8. (a) Saito, A.; Yamashita, T.; Mariko, Y.; Nosaka, Y.; Tsuchiya, K.; Ando, T.; Suzuki, T.; Tsuruo, T.; Nakanishi, O. *Proc. Natl. Acad. Sci. U.S.A.* **1999**, *96*, 4592; (b) Suzuki, T.; Ando, T.; Tsuchiya, K.; Fukasawa, N.; Saito, A.; Mariko, Y.; Yamashita, T.; Nakanishi, O. *J. Med. Chem.* **1999**, *42*, 3001.
9. Plumb, J. A.; Finn, P. W.; Williams, R. J.; Bandara, M. J.; Romero, M. R.; Watkins, C. J.; La Tangue, N. B.; Brown, R. *Mol. Cancer Ther.* **2003**, *2*, 721.
10. Finnin, M. S.; Donigian, J. R.; Cohen, A.; Richon, V. M.; Rifkind, R. A.; Marks, P. A.; Breslow, R.; Pavletich, N. P. *Nature* **1999**, *401*, 188.
11. Preliminary docking studies were done using HDLP X-ray structures.[10] See Refs. 17 and 18 for details of similar software and procedure used for HDAC1 homology modeling.
12. Wu, Z.; Rea, P.; Wickham, G. *Tetrahedron Lett.* **2000**, *41*, 9871.
13. Remiszewski, S. W.; Sambucetti, L. C.; Atadja, P.; Bair, K. W.; Cornell, W. D.; Green, M. A.; Howell, K. L.; Jung, M.; Kwon, P.; Trogani, N.; Walker, H. *J. Med. Chem.* **2002**, *45*, 753.
14. Baudy, R. B.; Fletcher, H., III; Yardley, J. P.; Zaleska, M. M.; Bramlett, D. R.; Tasse, R. P.; Kowal, D. M.; Katz, A. H.; Moyer, J. A.; Abou-Gharbia, M. *J. Med. Chem.* **2001**, *44*, 1516.
15. The recombinant HDAC enzymes, including HDAC1, 2, 3, 4, 5, 6, 7, 8, 9, 10 and 11, were produced by the Protein Biochemistry Group in S*BIO Pte Ltd. The assay was performed in a 96-well format using the BIOMOL fluorescent-based HDAC activity assay (BioMol International, L.P). The reaction mixture was composed of assay buffer, containing 25 mM Tris, pH 7.5, 137 mM NaCl, 2.7 mM KCl, 1 mM $MgCl_2$, 1 mg/ml BSA, tested compounds, an appropriate concentration of HDAC1 and 250 μM Flur de lys generic substrate. The fluorescence was detected at the excitation wavelength 360 nm and emission wavelength 460 nm using Tecan Ultra Microplate Detection System (Tecan Group Ltd, Switzerland). The analytical software, Prism 4.0 (GraphPad Software, Inc.) was used to generate IC_{50} values from the data. IC_{50}s for HDACs 2–11 were obtained by using analogous protocols but with appropriate adjustment of protein and/or substrate concentrations. The dissociation constant for binding of inhibitor to enzyme, the K_i, was calculated using the Cheng–Prusoff equation: $K_i = IC_{50}/(1 + ([\text{substrate}]/K_m))$.
16. Human colon cancer cell lines COLO 205, HCT116 and prostate cancer cell line PC3 were obtained from the American Type Culture Collection (ATCC; Virginia, USA). Human ovarian cancer cell line A2780 was obtained from the European Collection of Cell Culture (ECACC, Wilshire, UK). They were cultivated according to the supplier's instructions. After sub-confluent growth, cells were seeded in 96-wells plate at log growth phase. Before treatment, the plates seeded with solid tumor cells were incubated at 37 °C, 5% CO_2 for 24 h, while the plates seeded with liquid tumor cell lines were incubated at 37 °C, 5% CO_2 for 2 h. Treatment with compounds was carried out in triplicate wells for 96 h. Proliferation of solid tumor cells was monitored using Cyquant™ cell proliferation assay (Invitrogen Pte Ltd, Singapore), while proliferation of liquid tumor cells was monitored using CellTiter96 Aqueous one solution cell proliferation assay (Promega Pte Ltd, Singapore). Dose–response curves were plotted to determine the IC_{50} values using XL-fit (ID business solution Ltd, USA). IC_{50} is the concentration needed for inhibition of 50% cell proliferation of tumor cells.
17. Homology Modeling. The human HDAC1 protein sequence was downloaded from ExPASy (http://expasy.org). The *Aquifex aeolicus* Histone Deacetylase Like Protein (HDLP) sequence was downloaded from the Protein Data Bank (PDB, http://rcsb.org). The proteins were aligned using clustal W 1.83[18a] and the alignment manually edited. The secondary structure was predicted by Psipred[18b] and SSPro.[18c] The HDLP X-ray structure 1C3R[10] was downloaded from the PDB and used as a template. The homology model was built using Prime[18d] with standard settings. The homology model was finally subjected to 5000 steps of Steepest Decent minimization using MacroModel[18d] with OPLS-AA force field[18e] and the GB/SA solvation model.[18f] The HDAC1 homology model were prepared using the protein preparation wizard in Maestro[18d] with standard settings. Grids were generated using Glide version 4.0.217[18d] following the standard procedure recommended by Schrödinger. A metal constraint was included in the grid files in order to force the docked poses to form an interaction with the catalytic zinc.
18. (a) Chenna, R.; Sugawara, H.; Koike, T.; Lopez, R.; Gibson, T. J.; Higgins, D. G.; Thompson, J. D. *Nucleic Acids Res.* **2003**, *31*, 3497; (b) Jones, D. T. *J. Mol. Biol.* **1999**, *292*, 195; (c) Pollastri, G.; Przybylski, D.; Rost, B.; Baldi, P. *Proteins* **2002**, *47*, 228; (d) Prime, MacroModel, Glide and Maestro are products of Schrödinger, LLC, New York, NY (www.schrodinger.com).; (e) Kaminski, G. A.; Friesner, R. A.; Tirado-Rives, J.; Jorgensen, W. L. *J. Phys. Chem. B* **2001**, *105*, 6474; (f) Still, W. C.; Tempczyk, A.; Hawley, R. C.; Hendrickson, T. *J. Am. Chem. Soc.* **1990**, *112*, 6127.
19. For in vitro metabolic studies and pharmacokinetic data of compound 23 (SB639), see Venkatesh, P. R.; Goh, E.; Zeng, P.; New, L. S.; Xin, L.; Pasha, M. K.; Sangthongpitag, K.; Yeo, P.; Kantharaj, E. *Biol. Pharm. Bull.* **2007**, *30*, 1021.
20. Female athymic nude mice, 10–12 weeks of age, were implanted subcutaneously in the flank with 5×10^6 HCT116 cells. When the tumor reached a size of 100 mm^3, the mice were pair-matched prior to treatment. Tumor size was measured every second day and the tumor volume calculated as follows: tumor volume (mm^3) = $(\text{width})^2 \times \text{length}/2$. Compounds were dissolved in 10% *N*,*N*-dimethylacetamide (DMA)/10% Cremophore/80% water for ip route or 0.5% methylcellulose/0.1%Tween 80 for oral administration. Drugs were injected ip or orally administered via gavage everyday for a period of 21 days. Tumor growth inhibition (TGI) was calculated according to % $TGI = (C_t - T_t) * 100/(C_t - C_{t1})$ where C_t, the mean tumor size of the vehicle control group at time t; T_t, the mean tumor size of the treatment group at the time t; C_{t1} = the mean tumor size of the vehicle control group on the first day of treatment. Statistic analysis was done with one-way ANOVA followed by Dunnett's Multiple Comparison test (Prism 4.0).